JOURNAL OF MATERIALS SCIENCE 26 (1991) 3628–3638

Case study of dry mixing of δ-alumina ('Saffil') and silicon carbide ('Nicalon') fibres with a rapidly solidified Al–20Si–X powder

J. H. ter HAAR, J. DUSZCZYK
Laboratory of Materials Science, Delft University of Technology, Rotterdamseweg 137, 2628 AL, Delft, The Netherlands

Dry mixing of δ-alumina and SiC short fibres with a powder metallurgy processed aluminium alloy was performed aiming to provide a homogeneous powder material for subsequent consolidation. The major problem was to deagglomerate the clustered fibres, realizing that fibre aspect ratio should not be sacrificed to too large an extent during this first processing step. The mixing was tackled by co-processing the materials in a cylindrical tumbler operating either with or without ceramic balls. This comes down to applying two differing intensities of mechanical action. Particle size, shape, hardness and specific surface area of the materials were measured after ball milling, which was a successful deagglomeration process only for the δ-alumina fibre.

1. Introduction

Discontinuous fibre reinforced metal matrix composites (MMCs) generally exhibit lower mechanical properties than those with continuous fibre reinforcement. However, they possess a number of advantages: lower price of fibres, easier processing, and lower resulting degree of anisotropy. While much research on the production of MMCs has been focussed on the liquid metal routes, interest in powder metallurgy (PM) based production of MMCs is growing by rapid developments of new and promising fabrication technologies based on such techniques as dry and wet blending [1–7], ball milling [8], mechanical alloying [9], spray deposition [10] and injection moulding [11]. The combination of a wide choice of alloying compositions (control of microstructure) and ceramic reinforcement seems very favourable, as well as the relative ease of process adaptation.

The mixing of ceramic particles and metal powders does not generally pose big problems to reach uniformity of distribution, especially when wet mixing is used. Mixing problems do arise with the use of fibres or whiskers as they are mostly received in an agglomerated condition [1, 2, 12] or agglomerate during processing [3, 13]. Once fibres are dispersed in a metal powder, in general there is still a chance for segregation and subsequent agglomeration to occur during handling of the powder composite. These segregation processes are driven by differences in size, density, shape and resilience of particles [14]. Although several authors have reported on the successful application of wet methods of whisker/fibre/particle deagglomeration and mixing with metal powders [2, 5, 6], this approach was not contemplated because it is our opinion that it will deteriorate degassing behaviour. McLean and Dower [3] share the same ideology and use a proprietary method of dry mixing of Saffil® fibres and metal powders by employing a high-speed sieving mill at the cost of only small loss in fibre size.

This paper describes the dry mixing of a rapidly solidified (RSP) aluminium alloy powder with three forms of two types of commercially available ceramic fibres, via simple blending and via ball milling in a tumbler mixer.

2. Materials

2.1. Motivation of choice

There is a strong interest of especially the automotive industry in the high silicon content Al–20Si–X PM alloys, due to a combination of excellent mechanical performance, such as low thermal expansion, good thermal conductivity, improved wear resistance, good elevated temperature tensile properties and reasonably low production costs [15]. The properties of these hypereutectic alloy series (which cannot be produced by conventional casting techniques due to a too coarse microstructure) appear superior to the original Al–Si based casting alloys from which they were derived. The PM alloy chosen as matrix material for the present investigation belongs to this group and is currently in use for automotive applications.

The fibre reinforcements chosen are the two best known and most studied ones for use in composite materials. They have been proved to enable strong bonds with aluminium alloy matrices to be achieved. By combining these ceramics with the powder alloy it is aimed to achieve still better strength and wear properties.

0022–2461/91 $03.00 + .12

2.2. RSP aluminium matrix alloy

The matrix alloy of composition Al–20 wt % Si–3 wt % Cu–1 wt % Mg (ASCM20) is produced by an air-atomization process resulting in cooling rates of 10^4–10^6 K s^{-1}. The powder grains have a rounded irregular shape and most of them are finer than 150 μm (Table I, Fig. 1). The microstructure consists of primary Si crystals in an Al matrix with eutectically intergrown Si dendrites. Cu and Mg serve as age-hardening elements.

Chemical analysis of the total O content (by high-temperature oxide reduction) gives a value of 0.203 wt % [15]. Assuming that this is all surface oxide with a density of 3×10^3 kg m^{-3}, one arrives at an oxide layer thickness of ~ 10 nm. By Auger electron spectroscopic analysis, it was shown [15] that the surface layer of the powder is enriched in magnesium oxide.

As a measure of the grain size, the maximum chord length of a particle in an optical microscopic view was taken. This variable has a wide and skew distribution and has similarities to a log normal one. The geometric mean size of an ideal log normal distribution can be regarded as the 50% cumulative size (= median) on a logarithmic size scale. The present ASCM20 powder has a count-weighted geometric mean of 26 μm and a geometric standard deviation of 2.1.

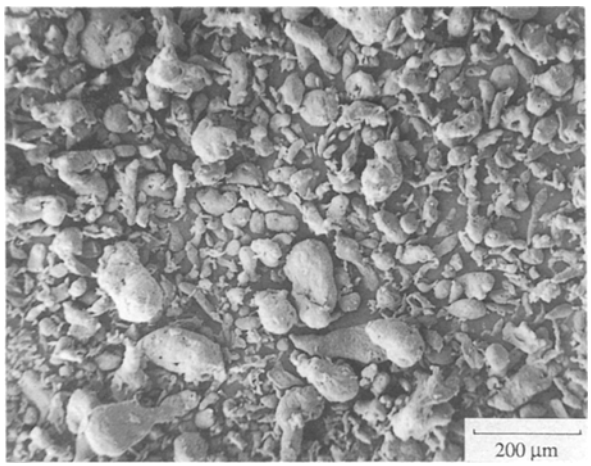

Figure 1 Scanning electron micrograph of air atomized powder ASCM20 showing the large spread in sizes and the irregular shapes of the particles.

2.3. Fibres

2.3.1. δ-alumina

Saffil δ-alumina fibres are produced by a unique solution-spinning process resulting in a very low level of "shot" (i.e. non-fibrous material). The material has an ultra-fine crystal size of mainly metastable δ-alumina (Table II). It contains 3%–4% silica which is added to inhibit transformation to α-alumina and prevent coarsening. It also assures better wetting with Al in molten metal MMC production routes. A fine (1–5 nm) silica-enriched layer is present on the surface of the fibre [16].

The Saffil RF grade fibre (pure δ-alumina) is commercially available in three main product forms; mat, bulk and milled, of which the last two were used in this study. The bulk form (Fig. 2), in large, often elongated, patches (10–200 mm) of wadding (clusters) consists of fibres with a length of 1–2 mm (Table II). The milled form used was type RF590 (Fig. 2), which consists of fibres that are milled and sized to a preselected range of lengths around 150 μm. Fig. 3 shows a scanning electron micrograph of the intricate entanglement of curved and branching fibres in a sample of Saffil bulk. It appears that long and thin fibres have the biggest curvature. The fibres have a relatively narrow distribution of diameters with a modal value of 3–4 μm (Fig. 4). The majority of fibres in the milled product is also present as clusters with sizes in the range 0.5–20 mm. Thus, the size of clusters appears to be a positive function of fibre size. The two forms of Saffil fibres were chosen in order to investigate the effect of starting fibre length on the final length of the fibres in the composites.

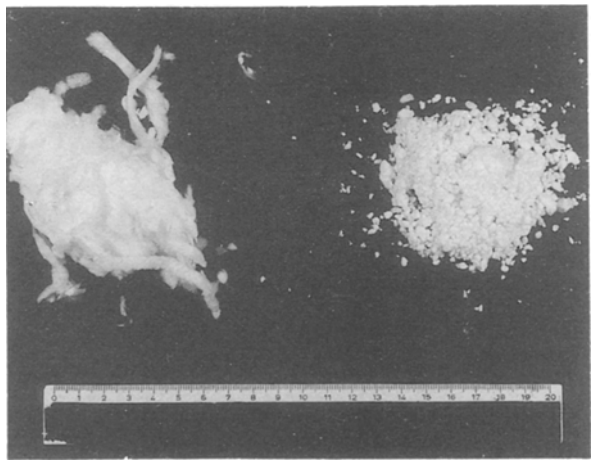

Figure 2 Macrograph of Saffil δ-Al_2O_3 fibre products (from left to right): bulk; milled (RF590).

TABLE I Data of matrix alloy, from the producer, unless stated otherwise

Trade name	ASCM 20[a]
Composition (wt %)	20 Si–3 Cu–1 Mg–0.3 Fe (bal. Al)
Density (kg m^{-3})	2.66×10^3
Tap density (kg m^{-3})	1.52×10^3 [b]
Mean particle size (μm)	26 (count-weighted, geometric)[b]
Particle shape	rounded, irregular
Specific surface (m^2 g^{-1})	0.18 [20]

[a] Showa Denko K.K., Japan.
[b] This study.

2.3.2. Silicon carbide

Nicalon® silicon carbide fibres are produced as continuous filaments by pyrolysing and subsequent heating to 1300 °C of a polycarbosilane polymer. They are heat treated above 1100 °C to stabilize the grain size at 3 nm and to improve high-temperature properties. The strength and elastic modulus of the fibre are constant up to 1000 °C.

TABLE II Data of fibre materials, from the producers, unless stated otherwise

Trade name	Saffil[a]	Nicalon[b]
Product form	grade RF: bulk, milled (RF590)	NCF-03M short chopped
Chem. composition	Al_2O_3/3%–4% SiO_2	SiC (/C/SiO_2)
Density (kg m^{-3})	3.3×10^3	2.65×10^3
Cryst. phase	mainly δ-Al_2O_3	–
Crystallite size (nm)	~ 30 [9]	3
Melting point (°C)	> 2000	–
σ_{uf} (MPa)	2000	2800
E_f (GPa)	300	200
Elongation (%)	0.67	1.6
Modal diameter (μm)	3–4[c]	14–15[c]
Modal length	bulk: 1–2 mm milled: 150 μm	3 mm
Spec. surface (m^2 g^{-1})	bulk: 0.51 [20] milled: 16.4 [20]	0.13

[a] ICI, Runcorn, UK.
[b] Nippon Carbon Company Ltd, Japan.
[c] This study.

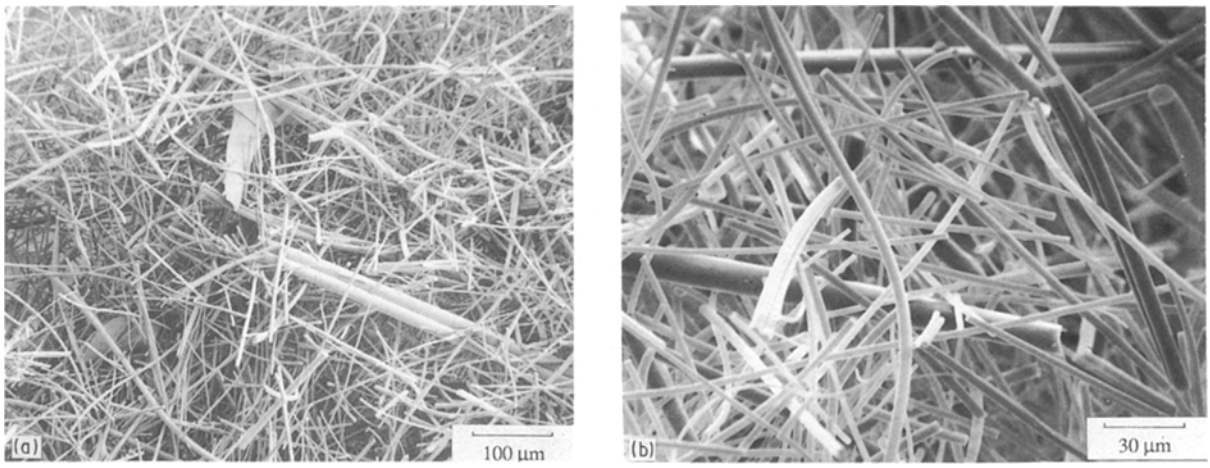

Figure 3 Scanning electron micrographs of the fibre network in a sample of: (a) Saffil bulk, (b) Saffil milled (RF590).

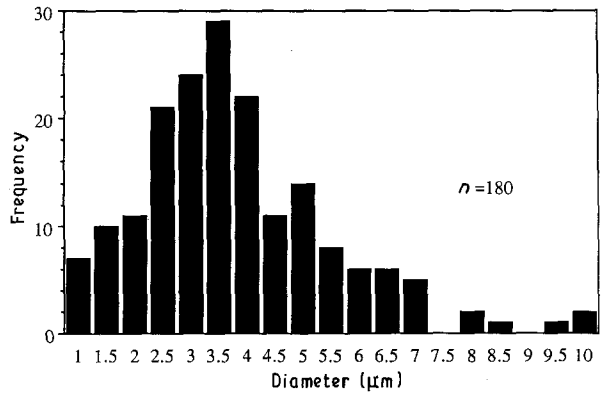

Figure 4 Saffil fibre diameter distribution by count obtained by microscopy of a plane section through some clusters.

Besides a majority of SiC, significant amounts of free C and excess Si combined with oxide are present, which are uniformly distributed across the fibre diameter [17].

Nicalon fibres come with or without sizing agents depending on application (for use in fibre-reinforced plastics (FRP), metals (FRM) and ceramics (FRC), and are commercially available in various product forms: continuous fibre (multifilament), chopped fibre, various woven products. In this study, chopped fibres (NCF-03M) of 3 mm length without sizing agent were used. Aggregates of fibres are present in this material (Fig. 5) in the form of originally aligned multifilament chops and secondary spheroidal fibre clusters (Fig. 6). The latter are most likely formed by tangling of individual fibres during agitation (handling) of the material. The fibres possess a modal diameter of ~ 14–15 μm (Fig. 7) and have a considerable amount of attached shot.

3. Methods

Two methods have been tested for their capability of deagglomerating and redistributing the three available forms of fibres in the matrix alloy. Employing a cylindrical tumbler mixer, the fibres and ASCM20 powder are inserted either without (blending) or with the addition of ceramic balls (ball milling) for more intense mechanical action. During blending, the powder will only experience internal shearing, whereas ball milling involves additional impact forces acting on the particles.

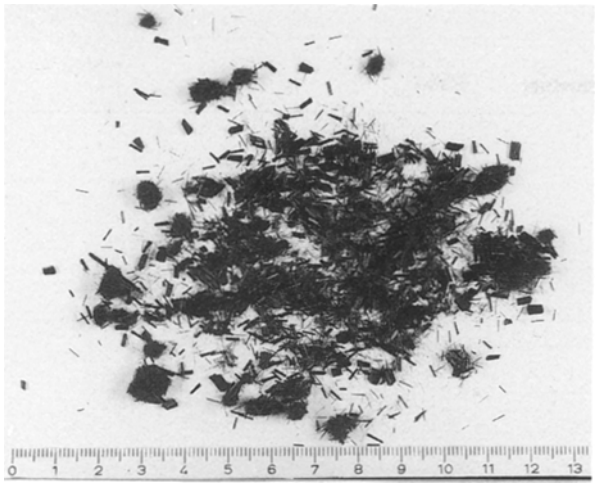

Figure 5 Nicalon SiC fibres in as-received condition. Note primary multifilament chops and secondary clusters.

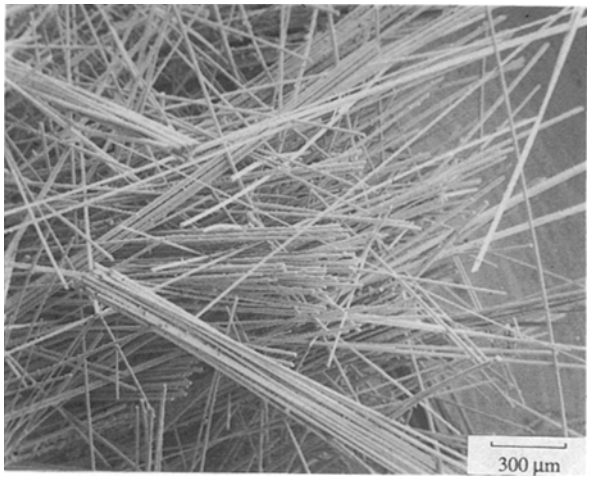

Figure 6 SEM close view of a Nicalon SiC cluster, also showing the tendency of fibres to stick parallel.

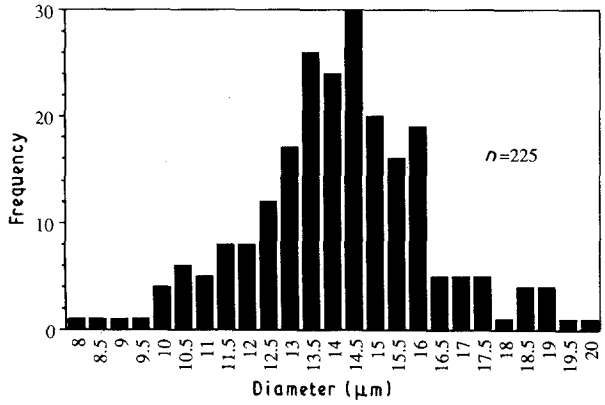

Figure 7 Nicalon fibre diameter distribution by count obtained by microscopy of a plane section through some multifilament fibre chops.

During ball milling, which is usually applied for breakage of brittle particles, balls will also exert forces on the present fibre clusters. This may give rise to fibre deagglomeration, in the worst case occurring by fibre breakage.

For the present application, a laboratory scale ceramic tumbler mixer was used with the following measures: diameter of mill, $D = 0.165$ m; length of mill, $L = 0.140$ m; diameter of ceramic balls, $d_b = 2.1 \times 10^{-2}$ m; density of balls, $\rho_b = 2.6 \times 10^3$ kg m^{-3}. The process parameters considered were [18]: fraction of mill filled by ball bed at rest (including formal bed porosity of 0.4) = fractional ball filling, J; fraction of mill volume filled by powder bed (including formal bed porosity of 0.4) = fractional powder filling, f_c; fractional speed (ratio between actual rotation speed, N, of a mill and the critical one, N_c, i.e. the theoretical speed at which the batch starts centrifuging; see below): $\phi_c = N/N_c$; milling time, t. An important derived parameter is the fractional ball porosity fill, i.e. the fraction of space between balls at rest that is filled with powder: $U = f_c/0.4J$.

An expression for the critical rotation speed N_c (at which zero mechanical energy is converted into the powder) is obtained by equating the gravity force on a ball on the mill wall against the radial centrifugal force [18]

$$N_c = K/(D - d_b)^{1/2} \quad (1a)$$

$$K = [30(2g)^{1/2}]/\pi = 42.3 \text{ m}^{1/2} \text{ min}^{-1} \quad (1b)$$

where g is the gravitational constant, 9.81 m s^{-2}.

The critical speed calculated with the present ball and mill dimensions and Equation 1 is 111.5 r.p.m. This appeared to be an underestimation for the real centrifuging speed. Practically, centrifuging batch motion can be inferred from the silent operation mode of a mill. The partly empirical formula of Rose and Sullivan [19] is more consistent with the observed behaviour

$$N_c = K_1/D^{1/2} \quad (2a)$$

$$K_1 = 50.8 \text{ m}^{1/2} \text{ min}^{-1} \quad (2b)$$

A critical speed of 125 r.p.m. calculated using Equation 2 is consistent with the experiment.

Depending on the fractional speed $\phi_c = N/N_c$, the degree of mill fill and the internal friction coefficient of the batch (balls and powder), the internal motion, can be dominated by either one of two distinct patterns. At low speeds, a cascading motion prevails in which the balls gently tumble down the inclined bed in parallel layers, whereas in cataracting motion at higher speeds more balls are ejected from the surface which describe parabolic paths [18].

Some basic aspects of milling including an account of the choice of parameters used for deagglomeration of clusters of fibres are discussed elsewhere [20].

In the size analysis of the fibres, only the length was taken into account because SEM observation confirmed that the diameter of individual fibres did not change by longitudinal fracture. Particle size was measured by transmitted light microscopy and on-line image analysis. Microscopic samples were prepared either by pipetting a drop of the suspension of powder in ethyleneglycol on a glass slide and placing a cover slide (for non-permanent samples, analysis of AB2, Table III) or by shifting a drop of the suspension of powder in butylacetate (with 2% collodion) with the

TABLE III Parameters during mixing experiments

Run	m (ASCM20) (g)	m (fibre) (g)	V (fibre)[a] (vol %)	J (%)	f_c (%)	U (%)	t (milling) (min)	Average N (r.p.m.)
S1	300	14.9	4.8 (C)	0	7	–	60[b]	110
AB1	300	18.6	4.8 (B)	0	7	–	156[b]	110
AM1	300	18.6	4.8 (M)	0	7	–	155[b]	110
S2	300	14.9	4.8 (C)	30	7	58	30[b]	110
AB2	300	18.6	4.8 (B)	30	7	58	300	110
AM2	300	18.6	4.8 (M)	30	13–7	108–58	10	110
A1	300	–	–	30	6	50	30	110

[a] (B) = Saffil bulk alumina fibre, (M) = Saffil milled alumina fibre, (C) = Nicalon siliconcarbide fibre.
[b] Clusters present at end of run.

edge of a glass slide on the surface of another glass slide (for permanent samples, analysis of AM2, Table III). The fibre size parameter determined was the maximum chord length which represents an underestimated fibre length when a fibre is curved.

4. Results

4.1. Blending

Blending at 110 r.p.m. for 60 min of 5 vol % Nicalon silicon carbide fibres with 300 g ASCM20 powder did not cause deagglomeration of the fibre aggregates (run S1, Table III). On the contrary, during the blending the clusters grew in volume and density, assuming perfect sphere shapes. Simple blending of 5 vol % Saffil bulk alumina fibre-reinforced composite was unsuccessful after an extended blending time of 156 min (run AB1, Table III). In the course of this process the size and volume of the large clusters of Saffil bulk fibre did not noticeably change. The mechanical action of the shearing powder mass could not cause any net deagglomeration.

When the blending experiment was performed with 5 vol % Saffil milled fibres (AM1, Table III), again no noticeable change of cluster size took place after 155 min. Again, the cluster structure appeared stable.

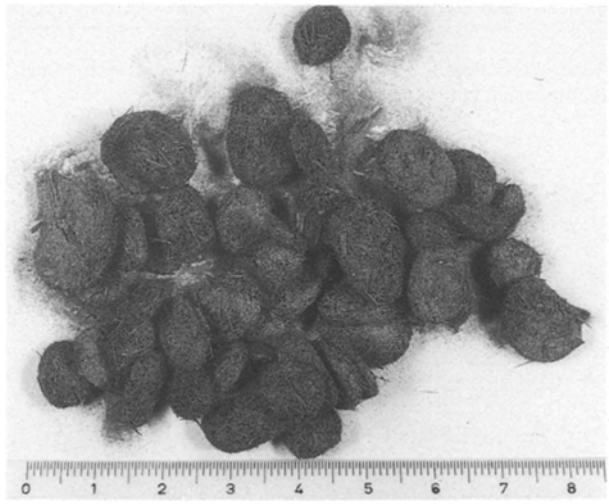

Figure 8 Large, compact and oblate clusters of Nicalon SiC fibre as obtained after milling (run S2). Note that the fraction of fibres shown is not representative for the actual volumetric composition.

4.2. Ball milling

Ball milling was performed with 99 ceramic balls of 21 mm diameter (run S2, AB2, AM2, Table III). A 5 vol % fibre reinforcement was used with 300 g ASCM20 powder. These gave lowest estimates of fractional ball porosity fill, U, of 58%. The higher values of U and f_c given for AM2 (Table III) are estimations of the initial values made with knowledge of the high specific volume (11.1 $cm^3 g^{-1}$) of the Saffil milled fibre material due to the clustering. The initial values for the experiments with the other fibres are likely two times higher than the ideal values (at perfect dispersion: 0.4 porosity) given. The mill rotation speed was set at a value of $\sim$ 110 r.p.m. ($\phi_c = 0.88$) providing a hypothetical cataracting motion of the batch.

4.2.1. SiC

The ball milling of 5 vol % Nicalon SiC fibre-reinforced composite (run S2) was not successful. A marked segregation occurred as was apparent from the presence of flattened clusters, being less in number, but larger and denser as compared to the original ones (Fig. 8). The mill/mixing method used in this study did not work for Nicalon SiC fibres for reasons that are discussed below.

4.2.2. δ-alumina (Saffil bulk)

Samples of 5 vol % Saffil bulk composite (run AB2) were analysed after 5, 10, 15, 30 and 300 min milling. By macroscopic observation it was found that after 5 min clusters up to 2 mm in size were still present (Fig. 9a) whereas they were absent after 10 min (Fig. 9b).

Fig. 10 shows the count weighted fibre size distributions of composite samples with homogeneous fibre distribution without clustering after 10, 15, 30 and 300 min milling (run AB2). In the sample taken after 5 min milling, fibre clustering was still observed; data were taken of dispersed fibres in the matrix powder.

Particle size distributions obtained by comminution (e.g. milling, grinding, crushing) often follow a log normal relation [21]. The statistic which characterizes at best the average of a log normally distributed population variable, is the geometric mean

$$x_g = \left(\prod x^{d\phi}\right)^{1/\phi} \quad (3)$$

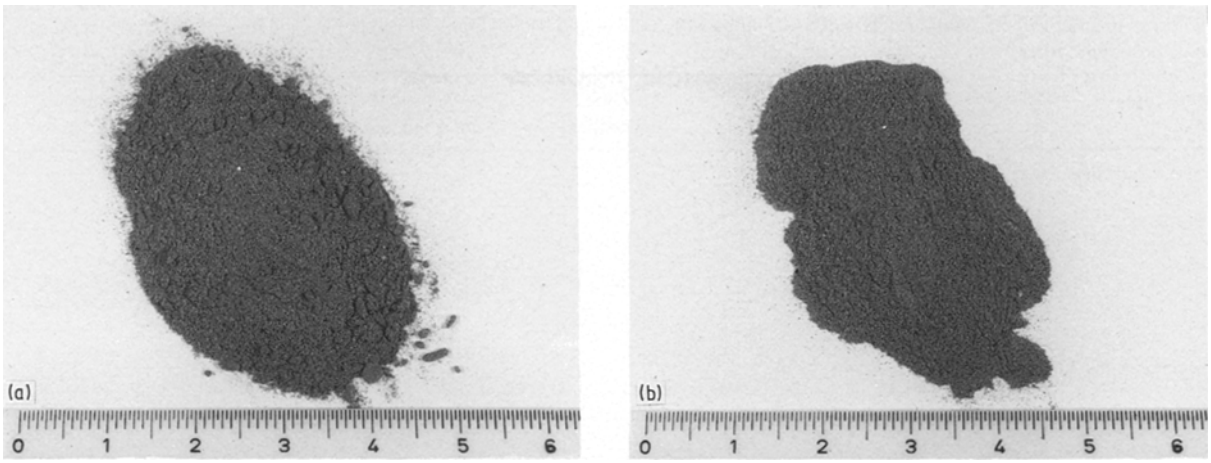

Figure 9 Macrographs of 5 vol % δ-Al_2O_3 composite (Saffil bulk, run AB2) ball milled for: (a) 5 min, exhibiting a granular texture build up by fibre clusters in the matrix, (b) 10 min, showing nearly smooth powder.

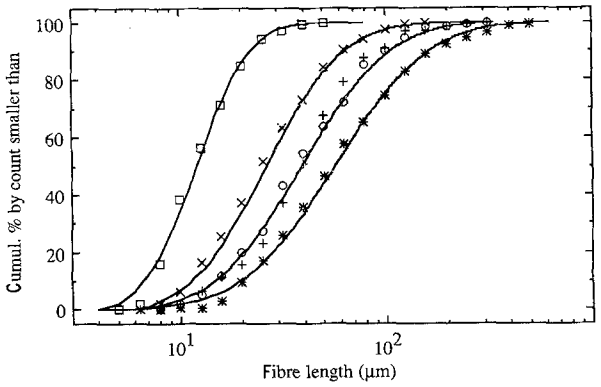

Figure 10 Fibre length distributions of δ-Al_2O_3 fibres in 5 vol % composite (Saffil bulk, run AB2) as a function of ball milling time. Log normal probability curves for the distributions at (*) 5, (○) 10, (+) 15, (×) 30, and (□) 300 min are drawn with their measured statistics l_g = 57, 39, 26, 12; σ_g = 2.3, 2.2, 2.0 and 1.6, respectively. *Fibre clusters present. n = (*) 166, (○) 151, (+) 178, (×) 188, (□) 160.

where $\phi = \sum d\phi$ and $d\phi$ is the frequency of occurrence of a value x. For an ideal log normal variable, x_g corresponds to the value with the highest expectation. As a measure for the spread around this value, the geometric standard deviation, σ_g, has to be used

$$\log(\sigma_g) = \left(\frac{\sum (\log x - \log x_g)^2 d\phi}{\sum d\phi} \right)^{1/2} \quad (4)$$

It can be looked upon as a ratio between two percentage points, e.g. $\sigma_g = (x_{84}/x_{16})^{1/2} = x_{84}/x_{50} = x_{50}/x_{16}$. For a log normal particle size distribution, Kapteyn's law states that the derived surface area, volume and higher moment distributions are also log normal with the same standard deviation and the following means [21]

$$\mu_j = \mu + 2.3026 j\sigma^2 \quad (5)$$

where j is the moment of the distribution and the relation is in terms of logarithms to the base 10. When the particles concerned are perfect cylinders, it can be proved that the geometric mean length by count and by weight are equal, by inserting the relation between fibre length and volume $l = V/C$ (where $C = \pi d^2/4$) in the equation for the differential of the log normal frequency curve

$$\frac{d\phi}{d \ln l} = \frac{1}{\ln \sigma_g (2\pi)^{1/2}} \exp\left[- \left(\frac{\ln l - \ln l_g}{2^{1/2} \ln \sigma_g} \right)^2 \right] \quad (6)$$

The present fibre size distributions can also be described according to the log normal relation. A statistical test for log normality was performed on the size data with the χ^2 (chi-squared) test for analysis of variance. All fibre size distributions of the 5 vol % composites (run AB2) except that after 300 min, pass the test successfully at a 5% level of unprobability (Table IV). The rejection of the hypothesis of log normality of the latter distribution is most likely due to its classification into too small a number of intervals, giving too rough an estimate of the χ^2 value.

In Fig. 10 ideal log normal curves obtained with the calculated mean and standard deviation of the distributions at 5, 10, 30 and 300 min are drawn. Although in general the cumulative relative frequency plot (as Fig. 10) does not reveal much detail of a distribution, its representation was chosen because of the ease of recognizing two important parameters of log normal distributions; the (geometrical) mean and standard deviation. Also, the percentage of fibres below a certain size can be read off quickly. Fig. 11 shows the variation of the geometric mean and standard deviation of the measured fibre length (l_g and σ_g, respectively) with milling time. The first data point concerns dispersed fibres in a matrix which contains fibre clusters (up to 2 mm in size). A drastic decrease of inferred overall mean fibre size is encountered in the initial stage (~ 10 min) of milling from 1000–2000 μm to 40 μm. The time necessary for the breakdown of macroscopic clusters is estimated to be in the region of 5–10 min, depending on the starting size of clusters. A milling time of 10 min provided a cluster-free composite powder with a geometric mean fibre length, l_g (aspect ratio), of 39 μm (13), and a geometric standard deviation, σ_g, of the distribution of 2.2. This implies that 84% of the fibres by count or by weight is smaller than 86 μm.

TABLE IV Results from χ^2 tests for analysis of variance between real and model (log normal) size distribution values: (a) milling with Saffil bulk fibres; (b) milling of only ASCM20 powder; (c) milling with Saffil milled RF590 fibres. The hypotheses of log normality are tested at a 5% level of probability of χ^2

Milling time (min)	Sample size, n	Degrees of freedom, f	χ^2-value determined	5% probability point of χ^2 at stated f	Log normality hypothesis
(a) Saffil bulk fibre length (run AB2)					
5	166	16	12.0	26.3	accepted
10	151	13	17.2	22.4	accepted
15	178	14	17.8	23.7	accepted
30	188	11	12.5	19.7	accepted
300	160	7	19.0	14.1	rejected
(b) ASCM20 particle size (run A1)					
0	364	15	48.1	25.0	rejected
10	239	13	19.9	22.4	accepted
15	368	14	45.7	23.7	rejected
30	363	15	29.3	25.0	rejected
(c) Saffil milled fibre length (run AM2)					
5	224	13	30.6	22.4	rejected

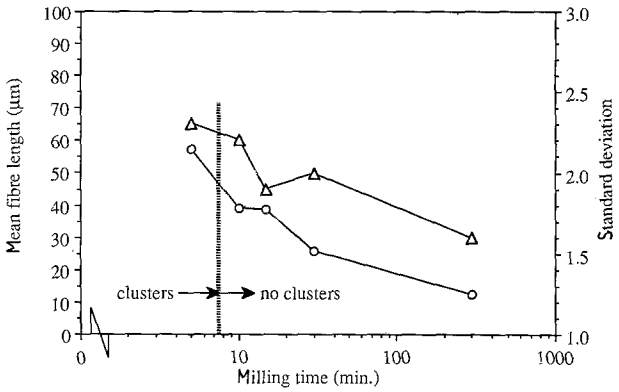

Figure 11 (○) Geometric mean and (△) geometric standard deviation (by count = by volume) of δ-Al_2O_3 fibres during run AB2. Clusters disappear in the region 5–10 min. Note that initial size of Saffil bulk fibres is 1000–2000 μm.

Figure 12 Scanning electron micrograph of 5 vol % composite with Saffil bulk (run AB2) after 10 min ball milling.

In Fig. 12 a scanning electron micrograph of the composite mixture with 5 vol % fibres at a milling time of 10 min is presented showing a homogeneous distribution of the reinforcement without clustering.

Ball milling can induce massive micro-forging of metal powder particles. When this occurs, a net grain shape change should take place. This was checked by determination of the ratio between the maximum and minimum (normal to maximum) ASCM20 particle chord length at different milling times. The effect of milling on the size distribution was also investigated. For these reasons, the ASCM20 powder was milled without fibres (run A1, Table III) to amplify the milling effect. Owing to a more severe milling action compared to the case when fibres are added (less damping), the effect is expected to be more pronounced. The results are presented in Figs 13 and 14. During run A1, the arithmetic mean aspect ratio of ASCM20 particles slightly drops while the standard deviation of the distribution remains the same. This means there is some particle deformation taking place. As the size analysis was performed by microscopy,

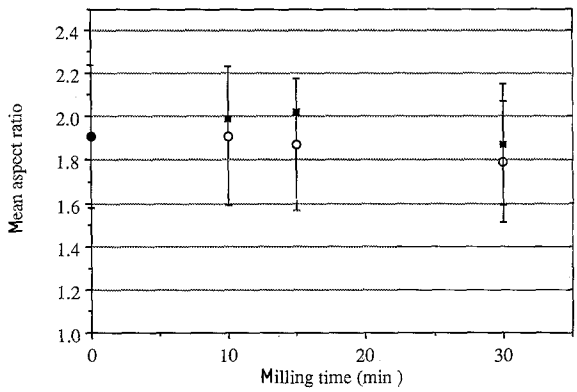

Figure 13 Mean aspect ratio of ASCM20 particles as a function of milling time. (○) Run A1 (only ASCM20), (*) run AB2.

possibly involving a preferred orientation of oblate particles (deformed) in the plane of view (view perpendicular to oblate axis), the decrease in aspect ratio can be explained by a flattening of particles.

From Fig. 14 it appears that the mean size and size

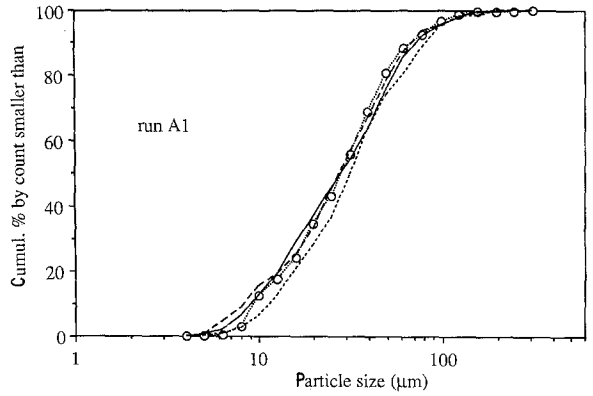

Figure 14 ASCM20 particle size distribution by count as a function of milling time. (· · · ○ · · ·) Initial, $n = 364$; (– – –) 10 min, $n = 239$; (— — —) 15 min, $n = 368$; (——) 30 min, $n = 363$.

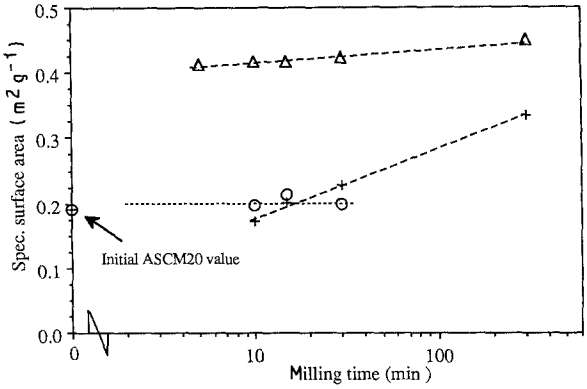

Figure 16 Specific surface area of powders during runs (○) A1 (ASCM20) and (+) AB2 (5 vol % composite). Also given are calculated values (△) for the fibres in run AB2 calculated with size data.

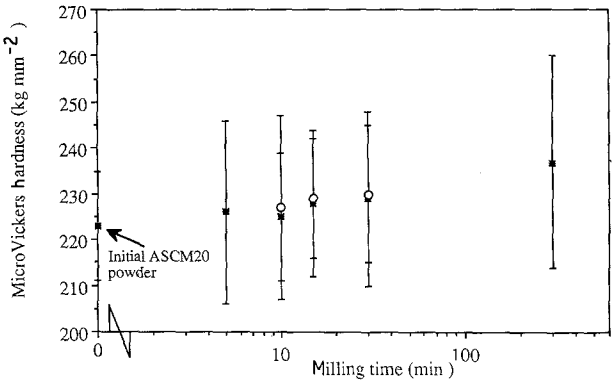

Figure 15 Hardness of ASCM20 particles (> 50 μm) as a function of milling time. Load: 245.2 mN. (*) Run AB2, (○) run A1.

distribution of the ASCM20 particles during milling (run A1) up to 30 min do not change significantly.

Table IV shows the results of the χ^2 test for log normality performed on the ASCM20 size distributions after milling. Particle size, as measured, cannot be generally classified as log normally distributed. Non-representative sampling could, however, be involved because one of the sampled populations does pass the test successfully.

It is assumed that during milling in the presence of fibres, there is also no demonstrable effect on particle morphology, as in the milling of only ASCM20 particles. The indication that some particle work hardening is taking place during the process is illustrated by the values of micro Vickers hardness measured with a standard load of 0.25 N (Fig. 15). Particles milled for 300 min seem to have a marked spread of hardness towards higher values but in the region up to 30 min the rate of increase of hardness is highest.

Fig. 16 presents the results of measurements of specific surface (BET) of the composite and loose ASCM20 powder as a function of the milling time. Milling of only the ASCM20 powder (A1) causes no significant change in specific surface up to 30 min. The mutual difference between the data points arises from powder sampling errors, possibly due to particle size segregation. The trend towards an increase of the surface area of the composite with milling time appears to be more consistent. It should be noted that the 5 vol % composite powder should theoretically give a higher specific surface compared to pure ASCM20 powder. The increase in specific surface area of the composite with milling time cannot be fully imputed to continuous breakage of fibres; the value of 0.45 $m^2 g^{-1}$ for the fibres at $t = 300$ min calculated from size distribution data is not compatible with the observed 50% increase in specific surface area of the composite. A contribution due to ASCM20 particle deformation must be included. Again, up to 30 min this increase is only small.

4.2.3. δ-alumina (Saffil milled RF590)

For the composite with 5 vol % Saffil milled fibres (run AM2), the same parameters, as established for Saffil bulk material, were applied (Table III). Samples for investigation were taken after 3, 5 and 10 min giving the optimal milling time of 5 min, after judgement of macroscopic homogeneity. These conditions yield a composite with mean fibre length, l_g (aspect ratio), of 38 μm (13) and standard deviation, σ_g, of 2.1. A scanning electron micrograph of the composite is shown in Fig. 17. The mean fibre size and size distribution as measured for the composite with the Saffil milled product are similar to those for the composite with the Saffil bulk fibre product as starting material (Fig. 18, Table V). However, the former fibre size distribution does not successfully pass the test for log normality (Table IV). It must be noted that two different sample preparation techniques were employed for the two composite powders (see section 3). The similarity suggests that the initial size of the fibres ball milled with the powder does not influence the final mean fibre length and aspect ratio (Table V). Only the milling time necessary to provide disintegration and homogeneous distribution of fibres in the matrix is shorter for the milled product. This difference in milling time is connected with a difference in total amount of work necessary to disintegrate the clusters in the two products.

With respect to their shorter milling time and easier handling (small initial cluster size), the Saffil milled fibres are, although shorter, more suitable for use in PM metal matrix composites.

TABLE V Saffil cluster and fibre size data before and after ball milling with ASCM20 powder. Milling until disappearance of clusters. Equal mill/fill parameters (runs AB2 and AM2, Table III)

Product type	Fibre length, initial (μm)	Cluster size, initial (mm)	Milling time (min)	Fibre length, final, l_g (μm)	S.D., final, σ_g	Fibre size red. fact.
Bulk	1000–2000	10–200	10	39	2.2	25–50
Milled	~ 150	0.5–20	5	38	2.1	~ 4

Figure 17 Scanning electron micrograph of 5 vol % composite with Saffil milled RF590 (run AM2) after 5 min ball milling.

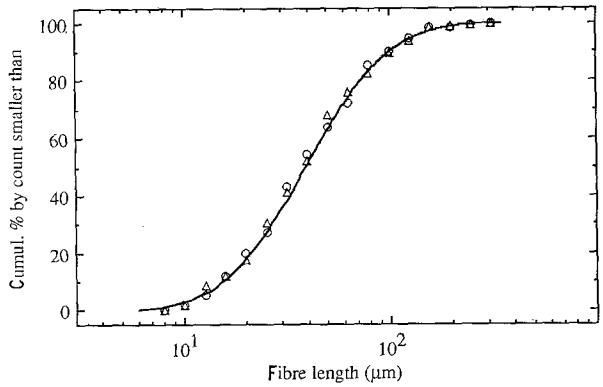

Figure 18 Size distribution of fibres in 5 vol % composites with (○) Saffil bulk (AB2) and (△) Saffil milled (AM2) at their optimal milling times (Table V). Log normal probability curve drawn with statistics $l_g = 39$ μm and $\sigma_g = 2.2$.

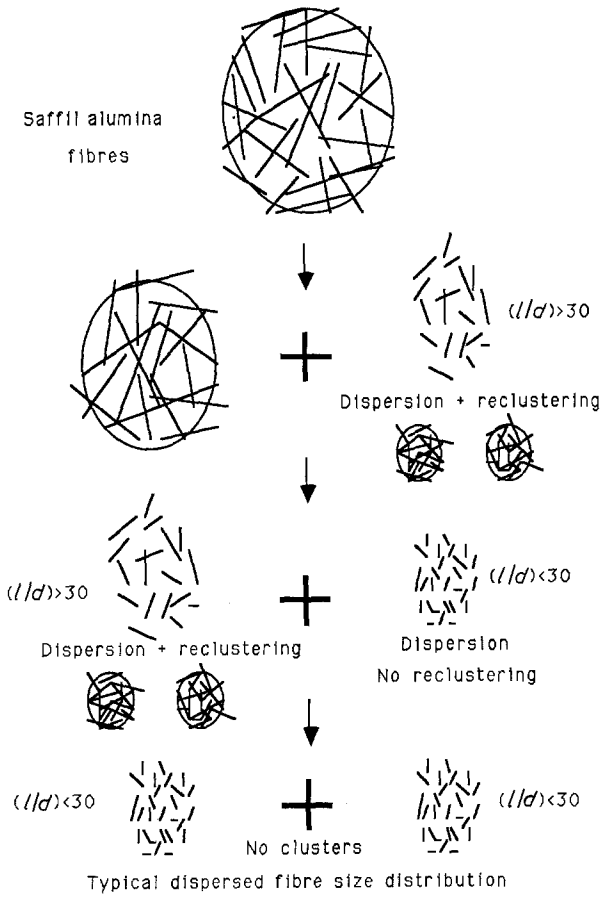

Figure 19 Model for the phenomenon of the Saffil fibre size reduction and the dispersion of fibres during the ball milling (elucidated in text).

5. Discussion

It has been postulated that a critical fibre length-to-diameter ratio of $l/d = 30$ exists above which fibres show agglomeration behaviour [3]. It is likely that a large size reduction of Saffil fibres takes place during the applied milling when clusters are disintegrated. An important observation is that the size of fibres dispersed in the matrix is already of the final order of magnitude ($\sim 10^2$ μm) at $t = 5$ min (in run AB2) when clusters (2 mm in size) are still present. This points to a mechanism in which fibres are released from the clusters through their individual fracture. The observed decrease in cluster size during milling (Fig. 9) points out that the process is steadily proceeding with time. There is, however, no definite answer to the degree of reclustering of the released fibres. A likely model which incorporates the concept of a critical length for clustering ($l/d = 30$) and the occurrence of reclustering is illustrated in Fig. 19. In this model a Saffil alumina fibre cluster releases some fibres on ball impact, after which the original cluster is left behind either reduced in size or in density. Depending on the size of the released fibres, clusters may form again of a size which is a function of fibre size. The model provides an explanation for the observed decreasing overall cluster size as well as for the similar fibre length distributions after our milling of the two differently sized Saffil fibre forms. Both milling of the Saffil bulk and the shorter Saffil milled fibre are compatible with the process displayed in Fig. 19; they yield one typical fibre size distribution after the disappearance of clusters because the fibres go through the same final trajectory of cluster size development. Compared to the dry mixing method applied by McLean and Dower [3] (blending and high-speed sieving) which results in a homogeneous mixture with fibres of

80–100 μm length, the present method yields a smaller mean fibre length and possibly a wider distribution of sizes.

The ability of the applied ball milling method to deagglomerate or rather break down δ-Al_2O_3 fibre clusters and not the SiC clusters, into the matrix powder can be explained on the basis of their material and geometrical properties.

When a fibre cluster in a ball mill is trapped between two colliding balls, it is easily seen that a few fibres will be hit directly, but a larger fraction will be indirectly stressed in bending. A minimum bend radius can be defined for a buckled fibre [22]

$$\lambda_{min} = \frac{E_f d_f}{2\sigma_{uf}} \quad (7)$$

where d_f is the fibre diameter, E_f the fibre Young's modulus, and σ_{uf} the fibre failure stress.

Also of importance is the flexibility of a fibre. The flexibility of a given material is a function of its elastic modulus and the moment of inertia of its cross-section. As a measure of flexibility of a fibre, the inverse of the product of bending moment, M, and radius of curvature, λ, can be used. It can be shown [23] that the flexibility $(1/M\lambda)$ is

$$\frac{1}{M\lambda} = \frac{64}{E_f \pi d_f^4} \quad (8)$$

The resilience of a fibre can be regarded as inversely proportional to flexibility. The flexibility of the Saffil δ-Al_2O_3 fibre is very much (an order of 2) higher than that of the Nicalon SiC fibre due to the difference in modal diameter (3 and 15 μm, respectively, Table II). The relatively small effect of the elastic modulus is illustrated by the fact that an SiC fibre of 3.3 μm has the same flexibility as the 3.0 μm δ-Al_2O_3 fibre (E_f = 300 and 200 GPa for Saffil and Nicalon fibres, respectively).

The values of the minimum bend radii, λ_{min}, for Saffil and Nicalon fibres (225 and 536 μm, respectively) are apparently in contradiction with the behaviour of fibre clusters during milling. When the flexibilities of the fibres are regarded the picture becomes clear. The Saffil material could be dispersed because the clusters responded on ball milling in a brittle way by breakage of fibres. One of the reasons why the clusters of SiC could not be deagglomerated was because the fibres did not respond by breaking. Unlike the firmly locked structure of curved and branching δ-Al_2O_3 fibres, the straight cylindrical SiC fibre shapes provide loose but flexible networks which deform on ball impact (Fig. 8). The combination of a high driving force for size segregation and the elastic relaxation forces on a ball–cluster impact can explain the intensified clustering.

Thus, the difference in mixing behaviour during milling must be attributed to the following effects.

1. The difference in the mechanical behaviour of clusters of the two materials due to differences in:

(a) fibre minimum bend radius (through σ_{uf}); the larger value for Nicalon SiC fibres though is not inconsistent with the results, as other factors mentioned also determine the behaviour;

(b) flexibility of the fibres (through E_f and d_f); the magnitudes of the moments acting on a δ-Al_2O_3 and a SiC single fibre just before fracture differ by a factor 525; the δ-Al_2O_3 Saffil fibres are extremely flexible compared to the Nicalon SiC fibres, which show relatively high resilience;

(c) fibre shape; firm locking of δ-Al_2O_3 clusters gives rise to mechanical stresses in fibres on collision with balls, whereas in the loose texture of SiC clusters fibres will only rearrange.

2. The difference in metal particle/fibre size ratio gives rise to severe segregation in the case of the large SiC fibres.

From this we can conclude that the use of larger or denser balls for stronger impact forces would not necessarily benefit the mixing of SiC fibres by ball milling.

6. Conclusions

1. Simple blending of the powders and fibres in a tumbler mixer was not successful in deagglomerating fibre clusters of both Saffil alumina products, bulk and milled, nor for the SiC Nicalon product. SiC clusters increased in size during blending.

2. Ball milling in a tumbler of 5 vol % fibre-reinforced material appeared capable of disintegrating clusters of δ-Al_2O_3 into singly dispersed fibres but caused increased cluster sizes of SiC fibres.

3. Optimum milling times are found for the two Saffil fibres (bulk and milled, 10 and 5 min, respectively) by macroscopically checking the presence of fibre clusters. The homogeneity of the fibre distribution at these points was good.

4. The length of Saffil alumina fibres after the applied milling times had drastically reduced. The fibre size distributions can, in most cases, be described by a log normal probability function.

5. At constant mill fill parameters, the measured final fibre size and size distribution in the 5 vol % δ-Al_2O_3 composite was virtually independent of initial size (Saffil bulk versus Saffil milled) which can be explained by a model incorporating reclustering of released fibres.

6. During the practised milling only minor and non-systematic changes in morphology and hardness of matrix aluminium alloy powders have been found at the applied milling times.

Acknowledgements

The stimulating discussions with Professors B. Scarlett and B. M. Korevaar are highly appreciated. The authors are grateful for the financial support of the Foundation for Technological Research (STW) and the Foundation for Fundamental Research of Matter (FOM).

References

1. A. P. DIVECHA, S. G. FISHMAN and S. D. KARMARKAR, *J. Metals* September **33** (1981) 12.
2. C. J. SKOWRONEK, A. PATTNAIK and R. K. EVERETT,

"Dispersion and blending of SiC whiskers in RSP Aluminium Powders", Report NRL-MR-5750 (Naval Research Laboratory, Washington, 1986) p. 699.
3. M. McLEAN and R. DOWER, in "Proceedings of the International Conference on Powder Metallurgy", Vol. 2, London, July 1990 (The Institute of Metals, London, 1990) p. 251.
4. Y. L. LIU, N. HANSEN, D. JUUL JENSEN, H. LILHOLT, P. NIELSEN and N. J. FEI, in "Proceedings of the Powder Metallurgy Conference", Vol. 3, San Diego, California, June 1989, edited by T. G. Gasbarre and W. F. Jandeska, MPIF/APMI (Princeton, New Jersey, 1989) p. 461.
5. A. DUNNING, N. J. E. ADKINS and G. P. YIASEMIDES, in "Proceedings of the International Conference on Powder Metallurgy", Vol. 2, London, July 1990 (The Institute of Metals, London, 1990) p. 298.
6. A. K. KURUVILLA, V. V. BHANUPRASAD, K. S. PRASAD and Y. R. MAHAJAN, *Bull. Mater. Sci.* **12** (1989) 495.
7. D. L. McDANELS, *Met. Trans. A* **16** (1985) 1105.
8. R. J. DOWER and M. McLEAN, *Int. J. Powder Metall.* **26** (1990) 69.
9. J. DINWOODIE and I. HORSFALL, in "Proceedings of the Sixth ICCM & ECCM", Vol. 2, London 1987, edited by F. L. Matthews, N. C. R. Buskell, J. M. Hodgkinson and J. Morton, (Elsevier Applied Science, London, 1987) p. 2.390.
10. M. GUPTA, F. MOHAMED and E. LAVERNIA, in "Metal and Ceramic Matrix Composites: Processing, Modelling and Mechanical Behaviour", edited by R. B. Bhagat, A. H. Clauer, P. Kumar and A. M. Ritter (The Minerals, Metals and Materials Society, Warrendale, PA, 1990) p. 91.
11. R. M. GERMAN and A. BOSE, *Mater. Sci. Engng* **A107** (1989) 107.
12. J. R. PORTER, *ibid.* **A107** (1989) 127.
13. J. M. YANG, W. H. KAO and C. T. LIU, *ibid.* **A107** (1989) 81.
14. J. C. WILLIAMS, *Powder Technol.* **15** (1976) 245.
15. J. L. ESTRADA and J. DUSZCZYK, *J. Mater. Sci.* **25** (1990) 886.
16. T. W. CLYNE, M. G. BADER, G. R. CAPPLEMAN and P. A. HUBERT, *ibid.* **20** (1985) 85.
17. G. SIMON and A. R. BUNSELL, *ibid.* **19** (1984) 3649.
18. L. G. AUSTIN, R. R. KLIMPEL and P. T. LUCKIE, "Process Engineering of Size Reduction: Ball Milling", Society of Mining Engineers, New York, 1984.
19. H. E. ROSE and R. M. E. SULLIVAN, "A Treatise on the Mechanics of Ball, Tube and Rod Mills" (Chemical Publishing Company, New York, 1958).
20. J. H. TER HAAR and J. DUSZCZYK, *Mater. Sci. Engng* **A, 131** (1991) in press.
21. G. HERDAN, "Small Particle Statistics" (Butterworth, London, 1960).
22. C. A. STANFORD-BEALE and T. W. CLYNE, *Comp. Sci. Technol.* **35** (1989) 121.
23. K. K. CHAWLA, "Composite Materials; Science and Engineering" (Springer Verlag, New York, 1987).

Received 10 October
and accepted 19 November 1990